CRISPR-Cas guided mutagenesis of chromosome and virulence plasmid in *Shigella flexneri* by cytosine base editing

Atin Sharma[a,b,c], Ruqiya Omer Aden[a,b,c], Andrea Puhar[a,b,c#], David A. Cisneros[a,b#]

[a]Department of Molecular Biology, Umeå University, Umeå, Sweden

[b]Umeå Centre for Microbial Research, Umeå University, Umeå, Sweden

[c]The Laboratory for Molecular Infection Medicine Sweden (MIMS), Umeå University, Umeå, Sweden

Running Head: programmable CRISPR-Cas mutations in *Shigella*

#Address correspondence to Andrea Puhar, andrea.puhar@umu.se, or David A. Cisneros, david.cisneros@umu.se

Andrea Puhar and David A. Cisneros contributed equally to this work as senior authors

Word count for Abstract: 242

Word count for Importance: 147

Word count for the main text (Excluding Acknowledgement, References, Figure legends, Tables, and Supplementary Material): 4780

Abstract:

Shigella is a Gram-negative bacterium that invades the human gut epithelium. The resulting infection, shigellosis, is the deadliest bacterial diarrheal disease. Much of the information about the genes dictating the pathophysiology of *Shigella*, both on the chromosome and the virulence plasmid, was obtained by classical reverse genetics. However, technical limitations of the prevalent mutagenesis techniques restrict the generation of mutants in a single reaction to a small number, preventing large scale targeted mutagenesis of *Shigella* and the subsequent assessment of phenotype. We adopted a CRISPR-Cas dependent approach, where a nickase Cas9 and cytidine deaminase fusion is guided by sgRNA to introduce targeted C→T transitions, resulting in internal STOP codons and premature termination of translation. In proof-of-principle experiments using an *mCherry* fluorescent reporter, we were able to generate loss-of-function mutants in both *E. coli* and *Shigella* with up to 100% efficacy. Using a modified fluctuation assay, we determined that under optimized conditions, the frequency of untargeted mutations introduced by the Cas9-deaminase fusion is in the same range as spontaneous mutations, making our method a safe choice for bacterial mutagenesis. Further, we programmed the method to mutate well-characterized chromosomal and plasmid-borne *Shigella* genes and found the mutant phenotype to be similar to that of the reported gene deletion mutants, with no apparent polar effects at the phenotype level. This method can be used in a 96-well plate format to increase the throughput and generate an array of targeted loss-of-function mutants in a few days.

Importance:

Loss-of-function mutagenesis is critical in understanding the physiological role of genes. Therefore, high-throughput techniques to generate such mutants are important for facilitating the assessment of gene function at a pace that matches system biology approaches. However, to our knowledge, no such method was available for generating an array of single gene

mutants in an important enteropathogen – *Shigella*. This pathogen causes high morbidity and mortality in children and antibiotic resistant strains are quickly emerging. Therefore, determination of the function of unknown *Shigella* genes is of utmost importance to develop effective strategies to control infections. Our present work will bridge this gap by providing a rapid method for generating loss-of-function mutants. The highly effective and specific method has the potential to be programmed to generated multiple mutants in a single, massively parallel, reaction. By the virtue of plasmid compatibility, this method can be extended to other members of Enterobacteriaceae.

Introduction

***S**higella* is a Gram-negative bacterium that belongs to the Enterobacteriaceae family. *Shigella flexneri* is the most prevalent species resulting in the disease – shigellosis or bacillary dysentery (1). Shigellosis is mostly a self-limiting disease in healthy adults but poses a major threat to children, elderly and the immunocompromised (2). With an annual death toll of 212,000, of which 63,713 are children below the age of 5, shigellosis is the deadliest bacterial diarrheal disease (3). Very low infection doses (10-100 bacteria), easy person-to-person spread and the acute inflammatory response are responsible for such high rates of incidence and mortality, especially in low- and medium-income countries (4). Being an invasive enteric pathogen, *Shigella* gains access to the intestinal epithelial cells by attaching and inducing its own uptake. Once inside the cells, it lyses the vacuole, replicates, and by using actin-based motility, disseminates to neighboring cells (reviewed in (5)). Virulence of *Shigella* requires a virulence plasmid-encoded type III secretion system (T3SS) which injects proteins into the host cell aiding the bacterium in establishment of infection through invasion, subversion of host defenses, and dissemination (reviewed in (6)).

We recently resequenced the genome of *S. flexneri* serotype 5a M90T, a widely used lab reference strain, and mapped global transcription start sites (7). Unsurprisingly, many transcription start sites led to identification of genes that await functional characterization to reveal new and interesting information about *Shigella* physiology. Loss-of-function mutagenesis, and subsequent assessment of phenotype, is a common and perhaps the most convenient way to determine the function of unknown genes. The classic allele replacement technique, first described decades ago by Datsenko *et al*. (8), is still the method of choice for targeted mutations in *Shigella* (9–11), but it has some limitations. Since the success of this technique is directly dependent on transformation of a linear DNA construct, the requirement of a large amount of DNA and electroporation limit its throughput. The two-step process,

allele replacement and subsequent removal, leaves a scar sequence which, if not optimized for being in-frame, results in polar effects that affect phenotype assessment (12). Although PCR-mediated construction of a linear DNA construct is easy, it requires expensive long primers and electroporation which adds to the final cost and acts as a technical bottleneck to increasing the throughput of mutagenesis.

CRISPR-Cas, a bacterial defense system against phages, has gained much attention for its use in genetic modifications (13). The *Streptococcus pyogenes* Cas9, the most commonly used protein for genome engineering, can be directed using guide RNA (gRNA) to introduce double-stranded (ds) DNA breaks (14). In eukaryotes, this is subsequently followed by DNA repair, resulting in generation of mutants, but in prokaryotes, a dsDNA break is lethal (15). Therefore, CRISPR-Cas based mutagenesis became the method of choice for targeted mutations in the eukaryotes, but its usage in prokaryotes was initially restricted to increasing the overall efficiency of allele replacement by positive selection (16, 17). However, later modifications resulted in the advent of base editors or catalytically impaired Cas9 proteins fused to deaminases, resulting in base substitution and, eventually, loss-of-function mutations (18, 19). These methods avoid dsDNA breaks and result in markerless mutations. Moreover, the requirement of plasmid borne sgRNA and effector proteins (Cas9 variants) eliminates the need of electroporation, thereby increasing the efficacy of the process, making it possible to multiplex or generate massively parallel mutations (20–22).

Here, we describe a CRISPR-Cas mediated base editing method, using an established cytidine base editor (20, 22) that can be programmed to generate loss-of-function mutations in *S. flexneri*. By mutating well-characterized *S. flexneri* genes of known phenotype/function, encoded on both the virulence plasmid and the chromosome, we show that the one-step method is easy, fast, and highly effective in inactivating genes. Utilizing this method, multiple genes in *S. flexneri* can be mutated in parallel, showing its great potential for high-

throughput mutagenesis.

Results

Construction of a two plasmid-based system for expression of sgRNA and nCas9-AID

As an effector protein, we selected a fusion of catalytically inactive Cas9 – nickase Cas9 ($nCas9^{D10A}$) and an ortholog of activation-induced cytidine deaminase (AID), previously described as an effective base editor in the Gram-positive industrial bacterium *Corynebacterium glutamicum* (22). The fusion protein is guided to the target gene by sgRNA (single guide RNA – 20 nt target-specific 'spacer' fused to a gRNA scaffold) where, within a window of -20 to -16 from the protospacer adjacent motif (PAM), the AID deaminates cytosine (C) to Uracil (U) and the nCas9 nicks the unmodified strand, resulting in its replacement and C→T (G→A on opposite strand) transition (Fig. 1A). This leads to conversion of internal CAG, CGA, and CAA codons on the coding strand or CCA on the non-coding strand into TAG, TGA, and TAA (STOP codons), premature termination of translation, and loss-of-function mutation.

We generated a medium-copy plasmid based on pSU19 (23), pnCas9-AID, to express nCas9-AID (Fig. 1B). The SacB encoding gene was cloned to facilitate curing of this plasmid (24). To express the sgRNA, we constructed a high-copy plasmid, pgRNA_AT, that uses a synthetic J23119 promoter. The *tac* promoter, used to drive the expression of nCas9-AID, is already known to function in *Shigella* (25). However, to determine J23119 activity in *Shigella*, superfolder GFP (sfGFP) with a synthetic ribosome binding site was cloned in pgRNA_AT (pgRNA-(R)-sfGFP) and transformed into *S. flexneri* (Supplementary Fig. S1). Expression of sfGFP, visualized by green fluorescence, showed constitutive activity of the J23119 promoter in *S. flexneri*.

To program a desired mutation, we used an online program – CRISPR-CBEI (26). It determines mutable sites and lists spacers required for the desired mutation in a target gene

(Fig. 1C). We synthesized spacers as oligos with overhangs complementary to the ends of BsaI digested pgRNA_AT to ensure directional cloning (Fig. 1D). The oligos were hybridized and phosphorylated prior to ligation and transformed in *E. coli* DH5α. All the transformants obtained carried the required recombinant plasmid as the cells transformed with non-recombinant plasmid are killed (22, 27).

Base editing effectively inactivates chromosomal genes in *E. coli* and *S. flexneri*

With optimal tools in hand, we tested our method by mutating a gene with an easy-to-read phenotype in *S. flexneri* and *E. coli* as a benchmark. We generated *attTn7*::*mCherry* insertion in *E. coli* MG1655 (*E. coli*::*mCherry*) and *S. flexneri* M90T 5a (*S. flexneri*::*mCherry*) using Tn7 transposition. We generated pgRNA_m2, pgRNA_m3, and pgRNA_m4 to introduce premature STOP codons in mCherry at the 69th, 114th, and 98th codon positions. We also constructed pgRNA-X, expressing a non-binding random spacer oligo.

We co-transformed *E. coli*::*mCherry* and *S. flexneri*::*mCherry* with pnCas9-AID or empty plasmid (pSU19) and with *mCherry*-targeting or control sgRNA plasmids (Fig. 2A). Co-transformants were selected as fluorescent colonies on selective medium containing glucose (Supplementary Fig. S2). To optimize the time and conditions necessary for mutagenesis, we plated actively growing cultures of *E. coli*::*mCherry* and *S. flexneri*::*mCherry*, with or without IPTG induction. To determine the frequency of mutation (Fig. 2B, C), we counted the resulting colonies and scanned them for red fluorescence (Fig. 2D, E).

In both species, the basal frequency of mutagenesis (no nCas9-AID and control gRNA-X) was zero (Fig. 2B-E, condition 1) and an *mCherry* targeting sgRNA alone (condition 2), or nCas9-AID with sgRNA-X, made no significant difference. This showed that gene-specific sgRNA alone or the nCas9-AID fusion bound to a control gRNA could not measurably introduce mutations. However, the frequency of mutagenesis was significantly higher than control, in both species, when nCas9-AID was expressed in presence of two out of three

mCherry-targeting sgRNA (Fig. 2B-E, conditions 4 and 6). Although the frequency was slightly lower in *S. flexneri* (median 85.7% and 66.7% as compared to 100% in *E. coli*), they were in the same order of magnitude irrespective of the addition of IPTG. This result shows that base-editing can be readily performed in *S. flexneri* with high efficiencies. However, a different effect was seen in case of sgRNA_m3. While the median frequency in *E. coli* was lower (87.8%) but in the same order as with sgRNA_m2 and sgRNA_m4, the median frequency in *S. flexneri* (8.3%) was not significantly different from the control condition (Fig 2C, condition 5). Addition of IPTG or longer incubation time did not improve the frequency (Fig. 2C, Supplementary Fig. S3). Together, these results indicated that sgRNAs had significant difference in their ability to target *mCherry* which shows species-dependent variation. Effective mutagenesis, however, could still be performed in both species, surprisingly, without chemical induction of nCas9-AID expression.

We also determined the bacterial titer (CFU/ml) for all the time points in each condition (Supplementary Fig. S3). The overall titer increased with time in both species, but there was no significant correlation across timepoints compared to the control conditions (condition 1). Therefore, with the present data, we cannot strongly conclude if carrying pgRNA derivatives, with or without pnCas9-AID, have specific effects on the titers. Only a small, but measurable, effect could be attributed to the addition of IPTG, which results in changes in growth rates or viability.

nCas9-AID is highly effective at undetectable levels

Differences in the efficacy of sgRNA_m3 in *E. coli* and *S. flexneri*, irrespective of IPTG induction, indicated that sgRNA, and not nCas9-AID expression, could be a factor responsible for the species-specific differences in the frequency of mutagenesis. To test this hypothesis, we transformed pgRNA-(R)-sfGFP into *E. coli* MG1655 and *S. flexneri*::*mScarlet* (*attTn7*::*mScarlet* in *S. flexneri*) and measured the sfGFP fluorescence over time. The

fluorescence was higher in *E. coli* (up to 6-folds) as compared to fluorescence in *S. flexneri*::*mScarlet* (Fig. 3A). This difference was confirmed at the single-cell level, when the green fluorescence was quantified by microscopy (Fig. 3B, Supplementary Fig. S4A). The expression of sfGFP from pgRNA-(R)-sfGFP was about four times higher in *E. coli* as compared to *S. flexneri* (Fig. 3C). This difference could be an outcome of several factors including, but not limited to, plasmid copy number, promoter activity, and sgRNA stability. This difference in sfGFP expression in the context of pgRNA_AT could explain differences in targeting efficiencies between *E. coli* and *S. flexneri.*

We had already determined that induction of the expression of nCAs9-AID was, surprisingly, not necessary for efficient mutagenesis. We wanted to determine if different levels of nCas9-AID correlated with *mCherry* mutagenesis guided by sgRNA_m2. Our results showed that in both *E. coli* and *S. flexneri*, *mCherry* was mutated despite nCas9-AID levels being below the limit of detection as determined by Western Blot (Fig 3D). nCas9-AID was detected upon IPTG induction, but accompanied by the appearance of bands below 100 kDa recognized by anti-Cas9 antibody, suggesting partial nCas9-AID degradation (Supplementary Fig. S4B). Interestingly, a previous study used dCas9-AID fused to a degron to decrease its expression (21). We seem to have achieved the same outcome, albeit inadvertently. These results indicate that the nCas9-AID fusion protein is not very stable but highly effective, nonetheless, even at barely detectable levels.

nCas9-AID expressing strains are not hypermutators

We suspected that leaky expression of nCas9-AID could alter the frequency of mutation at loci other than those targeted due to unspecific activity of the fused AID domain (28, 29). To test the basal mutation rate in *S. flexneri*, we performed the classic fluctuation assay using nalidixic acid (30). Point mutations in gyrase encoding gene, *gyrA*, render *Shigella* resistant to nalidixic acid (31). The frequency of appearance of such mutants can be used as a measure

172 of basal mutation rate. We designed a sgRNA (sgRNA-gyrA) that would cause a G→A
173 transition at position 259, resulting in Asp_{87} → Asn_{87} substitution and resistance to nalidixic
174 acid. *S. flexneri* strains carrying backbone plasmid pSU19, instead of pnCas9-AID, were used
175 to distinguish between the mutation rate at the *gyrA* locus in presence or absence of nCas9-
176 AID (Fig 4A). Mutagenesis was carried out as in case of *mCherry*, but in addition to spotting
177 on TSA plates, 10-fold serial dilutions of the cultures were also spotted on TSA plates
178 containing nalidixic acid and the resulting colonies were counted.
179 **T**he background rate of *gyrA* mutation in absence of nCas9-AID, as a proxy measure of
180 overall random mutation frequency, was in the order of 10^{-8} after 2 hours of incubation (Fig.
181 4B). It was not significantly altered when IPTG was added. Importantly, the expression of
182 nCas9-AID, in presence of a non-targeting sgRNA (sgRNA-X), also did not significantly
183 affect the mutation frequency. Even at later time points, the frequency of mutation for strains
184 expressing nCas9-AID with sgRNA-X was similar to those not expressing nCas9-AID at all
185 (Supplementary Fig. S4C). It was only in the presence of a *gyrA*-specific sgRNA (sgRNA-
186 gyrA) that nCas9-AID was able to introduce nalidixic acid resistance mutations at a higher
187 frequency. A nearly 5 log-fold increase in the frequency of mutation confirmed the specificity
188 of our method. The frequency of mutation, however, was not as high as with *mCherry*
189 mutagenesis, highlighting again that efficacy can depend on target genes and sgRNAs. The
190 low-level leaky expression, and even induced expression of nCas9-AID, was not mutagenic
191 by itself, probably due to the low stability of the fusion protein as observed by Western blot.
192 This also suggested that the probability of introduction of unwanted unspecific mutations by
193 nCas9-AID, under the conditions we tested, was in the same order of magnitude as
194 spontaneous mutations.

195 **Loss-of-function mutants generated by base editing have the same phenotype as gene**
196 **deletion mutants**

197 **E**ncouraged by our results, we decided to use our system to generate mutations in parallel in
198 well-characterized virulence genes on both the chromosome and the virulence plasmid and
199 verify their phenotype (Table 1, Fig. 5A). We mutated *mxiD* in *S. flexneri* and performed a
200 gentamicin protection assay to assess whether it had the same impact on invasion as reported
201 earlier (32, 33). Wild-type and *S. flexneri mxiD(Q323X)* (Q_{323} residue substituted with STOP
202 codon) were allowed to infect TC7 intestinal epithelial cells *in vitro* and the extracellular
203 bacteria were killed by gentamicin treatment. Bacterial invasion was quantified by lysing the
204 cells, to release intracellular bacteria that were protected from gentamicin, and spotting log-
205 fold dilutions of the lysates on TSA plates (Fig. 5B). WT bacteria successfully invaded TC7
206 cells, but we did not observe any invasion by *S. flexneri mxiD(Q323X)* (Fig. 5C). Since *mxiD*
207 mutants fail to assemble a functional T3SS, they are unable to secrete the T3SS substrates
208 (32). Indeed, we did not recover any secreted proteins in the supernatant of *S. flexneri*
209 *mxiD(Q323X)*, induced for secretion by Congo red (Fig 5D) (34).
210 ***i**csA* and *vacJ* have been reported to be necessary for intracellular dissemination of *Shigella*,
211 but are not involved in invasion (35, 36). We first verified that base-edited mutants *S. flexneri*
212 *icsA(Q59X)* and *S. flexneri vacJ(Q90X)* had no invasion defect (Fig. 5E). To assess
213 intracellular dissemination, we used the plaque formation assay, where cells are infected with
214 bacteria but the bacteria can only disseminate intracellularly due to the presence of
215 gentamicin in the medium (37, 38). Successful intracellular dissemination results in spread of
216 bacteria and subsequent cell death, which appears as a zone of clearance in the cell
217 monolayer (Fig 5F). Successful invasion and subsequent dissemination were evident in case
218 of WT *S. flexneri* as numerous plaques of similar diameter were observed (Fig. 5G).
219 However, no plaques were visible in case of *S. flexneri icsA(Q59X)* and *S. flexneri*
220 *vacJ(Q90X)*, even at higher MOIs, indicating an obvious dissemination defect.
221 **T**aken together, these results showed that the phenotype of the mutants generated by our base

editing method was consistent with that reported in the literature.

Base editing results in phenotypically non-polar mutations

Polar effects, or decreased expression of genes downstream of the site of mutation, are a common mutagenesis problem in bacteria for polycistronic transcriptional units (12). For example, polar effects of *icsB* mutation have been shown to impair intracellular dissemination in *Shigella* by affecting transcription of downstream *ipa* genes (9, 39, 40). We generated two *icsB* mutants (*S. flexneri icsB(Q32X)* and *icsB(Q237X)*) with the premature STOP codon introduced at two different sites (Fig. 5A). The *icsB* mutants had no apparent invasion defect (Fig. 5H) and there was no significant difference in the number and size of the plaques as compared to WT bacteria (Fig. 5G and 5I). This indicated that base edited *icsB* mutant might be non-polar.

To verify this effect at the mRNA level, we additionally mutated *ipgB*, a gene upstream *ipaC*, by constructing two *ipgB* mutant strains [*S. flexneri ipgB(Q44X)* and *S. flexneri ipgB(Q190X)*]. We determined the expression of *icsB*, *ipgB* and *ipaC* by qPCR (Fig. 6A). Two-way analysis ANOVA showed no significant differences between the transcription of *ipgB* and *ipaC* between wild-type *S. flexneri* and the four *icsB* and *ipgB* mutants (Fig. 6B). Moreover, no mutation showed significant differences compared to wild-type *S. flexneri* when transcription of *ipgB* or *ipaC* was analyzed individually (Supplementary Fig. S4D). As expected, no effect was observed at the protein level, assessed by comparing the secretion of IpaC (Fig. 6C). Although a loss-of-function mutation of *ipgB* has been reported to be 50% less invasive (41), we did not observe this decrease, mainly because this reduction is within experimental error in our hands (Fig. 6D). We did observe a significant effect on the levels of *icsB* transcription (Supplementary Fig. S4D), particularly for the *S. flexneri icsB(Q32X)* mutant, which is consistent with our previous report (42) that some mutations, including premature STOP codons, can decrease mRNA levels without affecting observed phenotypes.

247 Altogether, these results showed that base-edited premature STOP codon mutations did not
248 result in any observable polar effects, at least at the phenotype level.

249 ## Discussion

250 **F**unctional characterization of genes is a primary step in understanding the physiology and
251 pathogenesis of microbes, which is made possible by powerful tools such as high-throughput
252 reverse genetics (43). However, the success of this approach is entirely dependent on the
253 ability to generate loss-of-function libraries with an equally high throughput (44). Using a
254 two-plasmid system and substituting electroporation with chemical transformation we were
255 able to increase throughput ensuring pure colonies of several desired mutants prepared in
256 parallel, in just 5-6 days from the receipt of spacer oligos (Supplementary Fig. S5). The use
257 of type II restriction enzyme BsaI not only ensures directional cloning of spacer oligos but
258 also provides the advantage that the parent plasmid needs to be digested only once for all
259 cloning reactions. Furthermore, even for the gRNA that showed no significant frequency of
260 mutation (sgRNA_m3) compared to the control, the reaction yielded a workable number of
261 mutant colonies.

262 **A**lthough high frequency of mutation was achieved in previous studies by combining the
263 expression of catalytically inactive Cas9, dCas9-AID, and a uracil DNA glycosylase inhibitor
264 (21, 46), we avoided using this combination as the uracil DNA glycosylase inhibitor can
265 potentially induce hypermutation, owing to its ability to impair DNA repair (47). In our case,
266 the apparent low stability of nCas9-AID and combined expression with a sgRNA, targeting or
267 non-targeting, might have decreased the availability of free apo-nCas9-AID, preventing it
268 from binding to non-specific sites on genomic DNA (48) and introducing unwanted,
269 potentially toxic mutations. Since the virulence plasmid is not necessary for bacterial
270 survival, improved yield of mutants by counter-selecting the non-modified cells using
271 CRISPR-Cas9 and recombineering methods together, is not applicable to mutation of

plasmid-borne genes (16, 17). However, we were able to mutate plasmid and chromosomal genes in *S. flexneri* in parallel using the same strategy and workflow.

It is now clear that polar effects are prevalent even in well-characterized systems such as the Keio collection (49). Therefore, even if we did not observe any polar effects at the phenotype level in this study, we observed potential changes in mRNA abundance and recommend that such effects are taken into account while generating base-edited mutants, in equal manner as for any other mutagenesis strategy.

In addition to generating parallel single gene mutations, a spacer oligo library can be cloned into pgRNA in a single reaction resulting in a pgRNA plasmid library. This library can be transformed into bacteria expressing nCas9-AID, generating an equally large pooled library of loss-of-function mutants. Since the pgRNA (ColE1-derived origin) propagates stably (50), cloned spacer oligos can function as barcodes, aiding in high-throughput screening of gene function (51) and base editing can be subsequently used for targeted mutagenesis of selected candidates.

Despite many apparent advantages, the most obvious limitation of the base editing method is the availability of mutable sites in a particular gene. Certain genes, for example *mxiD* in this study, have only one mutable site. As seen from our results, certain sgRNAs are more effective than others and not having any alternative, therefore, can be limiting. However, with the discovery of Cas9 variants with varying PAM specificity, there is a possibility of combining them with deaminases to expand the arsenal of effector proteins to overcome this limitation (52). Altered PAM specificity can also address another possible limitation in form of the usage of amber codon for termination. Amber codon is only rarely used for termination of essential genes and is often a suboptimal STOP codon (53).

In conclusion, we have successfully adapted a programmable CRISPR-Cas9 base editing method to generate loss-of-function mutants in *S. flexneri* and *E. coli*. This method can allow

functional characterization of unknown *S. flexneri* genes by high-throughput reverse genetics and could be extended to other members of Enterobacteriaceae owing to plasmid and promoter compatibility.

Methods

Bacterial strains, cells, and culture conditions

Bacterial strains, plasmids, and cells used in this study have been summarized in the Supplementary Table S1. All *E. coli* strains were grown in LB, *S. flexneri* in TSB, and TC7 cells were gown in DMEM containing 10% FBS, non-essential amino acids and penicillin-streptomycin. For maintenance of plasmids in *E. coli*, chloramphenicol and carbenicillin were used at 25 µg/ml and 100 µg/ml, respectively. In case of *S. flexneri*, the concentration was 15 µg/ml and 50 µg/ml, respectively. Spectinomycin was used at 50 µg/ml. *S. flexneri* colonies were selected on agar plates supplemented with 0.01% Congo red.

Construction of fluorescent strains

Fluorescent strains of *E. coli* and *S. flexneri*, constitutively expressing *mCherry* (and *mScarlet-i* in case of *Shigella*) from the chromosome, were constructed using Tn7-mediated transposition (54, 55). The detailed methodology is mentioned in Supplementary Methods S1.

Plasmid construction

All the oligos used for recombinant procedures are mentioned in Supplementary Table S2. pgRNA_AT was generated by combining parts from pgRNA-ccdB and a pBluescript SK variant that lacks the BsaI site in the β-lactamase gene (22). pnCas9-AID was generated by combining parts of pSU19 and pdCas9-AID by *in-vivo* assembly (IVA) cloning (22, 56). Plasmid construction is explained in detail in Supplementary Methods S1.

Guide RNA design and cloning

The guide RNA for mutagenesis were designed using the program CRISPR_CBEI (26) (Supplementary Table S2). Details of cloning and guide RNA design are mentioned in

Supplementary Methods S1.

Mutagenesis

pnCas9-AID and respective pgRNA were co-transformed in ultra-competent *E. coli* using the heat shock method (57). The co-transformants were selected on LA plates supplemented with chloramphenicol, carbenicillin, and glucose. Since co-transformation was not very efficient in *S. flexneri*, pnCas9-AID and various sgRNA plasmids were sequentially transformed.

Bacteria carrying both plasmids were grown overnight at 37°C in broth supplemented with chloramphenicol, carbenicillin, and glucose. The overnight culture was diluted 100 times in fresh medium and the bacteria were grown till OD_{600} = 0.2. 1 mM IPTG was added to overexpress nCas9-AID and the cultures were incubated at 37°C for further 2 hours (longer incubation times were tested in case of *mCherry* and *gyrA* mutagenesis). 10-fold serial dilutions of the cultures were made in sterile PBS and 10 µl of each dilution was spotted on agar plates containing no antibiotics. For *gyrA* mutagenesis, the agar plates were supplemented with nalidixic acid (30 µg/ml) and in addition to 10-fold dilutions, a 10-fold concentrated culture was also spotted. The agar plates were incubated overnight at 37°C and the colonies were enumerated. The plates were imaged in a Typhoon scanner (GE Healthcare) to determine fluorescence. Four random colonies were selected in each case to verify mutation by PCR and sequencing.

Fluorescence measurement and microscopy

Overnight cultures of *E. coli* MG1655 and *S. flexneri*::*mScarlet* carrying pgRNA-(R)-GFP were diluted 100 times in fresh medium containing carbenicillin. 100 µl of culture was pipetted into different wells of a 96-well plate and the fluorescence (Ex: 480 nm and Em: 510 nm) and OD_{600} was measured simultaneously every 10 min in a SPARK multimode plate reader (Tecan) at 37°C. After 3 hours of incubation, 10 µl of both cultures were mixed in a tube and spotted onto a thin agarose pad on a glass slide. Microscopy images were taken

347 using widefield microscope (Nikon) with DIC, Texas red, and FITC filters. The images were
348 given false colors and fluorescence quantification was performed using ImageJ.

349 **Immunodetection of nCas9-AID**

350 Bacteria were cultured similarly to the mutagenesis assay but instead of spotting dilutions on
351 agar plates, 10 ml of cultures were pelleted by centrifugation and resuspended in 250 µl of 1X
352 Laemmli buffer. The samples were boiled and resolved on 10% SDS-PAGE. The gels were
353 stained using SimplyBlue stain (ThermoFisher) or used for transfer of proteins onto PVDF
354 membranes (GE Healthcare). Probing was done using anti-Cas9 primary antibody
355 (ThemoFisher, PA5-90171) at 1:20,000 dilution and HRP-conjugated anti-rabbit secondary
356 antibody (Abcam) at 1:40,000 dilution. The blot was developed using ECL reagent (Cytiva)
357 and imaged using Amersham imager 680 (Sigma Aldrich).

358 **Bacterial invasion assay and plaque formation assay**

359 **T**he ability of bacteria to invade epithelial cells was determined by gentamicin protection
360 assay as described earlier (33). All mutant *Shigella* strains were transformed with pAfaE, a
361 derivative of pIL22 (58) expressing AFA I adhesin. Plaque formation assay was performed as
362 described in (38) with modifications as follows. TC7 cells were infected at an MOI of 1:500
363 (bacteria:cells) and additionally at 1:150 for *vacJ* and *icsA* mutants. The infected cells were
364 incubated for 48-72 h before fixation and staining.

365 **Secretion assay**

366 **S**ecretion assays were performed as described earlier with modifications (59). Overnight
367 cultures of bacteria were diluted 200 times and were grown till OD_{600} = 0.5. Cells were
368 collected from 4 ml culture, by centrifugation, and washed twice with PBS. The pellet was
369 finally resuspended in 1 ml prewarmed PBS containing 0.01% Congo red and incubated for 1
370 hour at 37°C. Bacteria were separated by centrifugation and the proteins in the supernatants
371 were precipitated at 4°C for 10 min using 20% trichloroacetic acid. 1 mg/ml solution of BSA

372 was used as a control for precipitation. The precipitated proteins were washed twice with ice-
373 cold acetone and resuspended in Laemmli buffer before being resolved on 12%
374 polyacrylamide gel. The gel was soaked overnight in 50% ethanol to remove Congo red and
375 rehydrated gradually. The gel was stained with SimplyBlue SafeStain (ThermoFisher) to
376 visualize the proteins.

377 **96-well mutagenesis**

378 **5**0 µl chemically competent *S. flexneri* carrying pnCas9-AID were pipetted into wells of a
379 pre-chilled 96-well plate. sgRNA plasmids were added to individual wells and transformed
380 by the heat-shock method. 150 µl of recovery medium (SOC) was added to each well and the
381 plate was incubated at 37°C for 1 h. 100 µl of cell suspension and $1/10^{th}$ dilution from each
382 well were spread onto selective plates. The plates were incubated overnight at 37°C and
383 single colonies were picked up for mutagenesis. In a 96-well deep-well plate (Eppendorf),
384 single colonies were inoculated in 500 µl of TSB with antibiotics and grown overnight at
385 37°C. 10 µl of overnight culture was added to 500 µl of fresh medium in a new 96-well deep
386 well plate, which was incubated till OD_{600} = 0.2. 1 mM IPTG was added to the wells and the
387 plate was incubated for another 2 h before serial dilutions (10 µl of 10^{-5} and 10^{-6} dilution) of
388 the cultures were spotted on Congo red plates. The plates were incubated at 37°C overnight
389 and single colonies were checked for desired mutation by colony PCR and DNA sequencing.

390 **qPCR analysis**

391 **T**otal RNA extraction and qPCR were performed as previously described, with minor
392 modifications (42, 60). Bacteria were grown similarly to the mutagenesis experiment but
393 instead of spotting the dilutions, the cultures were treated with ice-cold Stop Solution (95%
394 v/v ml of ethanol, 5% v/v ml of phenol pH 4) for 30 min on ice. The cells were then collected
395 by centrifugation and stored at -80°C. cDNAs were subsequently prepared with random
396 hexamer primers using a first strand cDNA synthesis kit (ThermoFisher). To analyze the

397 expression of *icsB, ipgB, ipaC*, and two housekeeping genes, *hcaT* and *cysG* (61), we
398 designed specific oligonucleotides (Supplementary Table S2). To analyze qPCR data, we
399 used the iQ5 optical system software (Bio-Rad) and obtained the Ct with default settings. We
400 manually verified that changes in the threshold did not affect or bias the results. To normalize
401 the data, the average Ct value of the two housekeeping genes was used to calculate a ΔCt for
402 the gene of interest. Controls with no reverse transcriptase were also analyzed to exclude the
403 presence of contaminating genomic DNA fragments.

404 **Acknowledgement**

405 AP acknowledges funding from Swedish Research Council (Vetenskapsrådet) grant number
406 #2016-06598, institutional support from Umeå University, Knut and Alice Wallenberg
407 Foundation grant KAW 2015.0225, and Carl Kempe Foundation grant JCK-2031.3. DAC
408 acknowledges support from the Carl Tryggers Stiftelse för Vetenskaplig Forskning grant CTS
409 18-65 and the Kempestiftelserna grant SMK 1860. DAC was supported in part also by funds
410 from the Novo Nordisk Foundation (Grant no. NNF17OC0026486) awarded to Dr.
411 Emmanuelle Charpentier at MIMS, The Laboratory for Molecular Infection Medicine
412 Sweden). AS was funded by MIMS Excellence by Choice Postdoctoral Programme stipend
413 under the patronage of Emmanuelle Charpentier grant SMK-1532.2 and Svenska Sällskapet
414 för Medicinsk Forskning (SSMF) Postdoctoral grant PD20-0022.
415 The authors are thankful to Yu Wang and Jibin Sun, Tianjin Institute of Industrial
416 Biotechnology, Chinese Academy of Sciences, Tianjin, China for kindly gifting the pnCas9-
417 AID-YU and pgRNA-ccdB plasmids; Javier Pizarro-Cerdá, Institut Pasteur, Paris, France for
418 providing pSU2.1rp-mCherry plasmid; and Justin L. Sonnenburg, Stanford University School
419 of Medicine, Stanford, USA for providing sfGFP carrying *Bacteroides thetaiotaomicron*
420 strain.

421 Author contributions as per CASRAI are as follows. Conceptualization: AS, AP, DAC.

422 Formal analysis: AS, ROA, DAC. Funding acquisition: AS, AP, DAC. Investigation: AS,
423 ROA. Methodology: AS, ROA, AP, DAC. Project administration: AP, DAC. Resources: AP,
424 DAC. Supervision: AP, DAC. Visualization: AS, ROA. Writing – original draft: AS. Writing
425 – reviewing and editing: AP, DAC, AS.

426 **References**

427 1. Kotloff KL, Nataro JP, Blackwelder WC, Nasrin D, Farag TH, Panchalingam S, Wu Y,
428 Sow SO, Sur D, Breiman RF, Faruque AS, Zaidi AK, Saha D, Alonso PL, Tamboura B,
429 Sanogo D, Onwuchekwa U, Manna B, Ramamurthy T, Kanungo S, Ochieng JB, Omore
430 R, Oundo JO, Hossain A, Das SK, Ahmed S, Qureshi S, Quadri F, Adegbola RA,
431 Antonio M, Hossain MJ, Akinsola A, Mandomando I, Nhampossa T, Acácio S, Biswas
432 K, O'Reilly CE, Mintz ED, Berkeley LY, Muhsen K, Sommerfelt H, Robins-Browne
433 RM, Levine MM. 2013. Burden and aetiology of diarrhoeal disease in infants and young
434 children in developing countries (the Global Enteric Multicenter Study, GEMS): a
435 prospective, case-control study. Lancet 382:209–222.

436 2. Anderson M, Sansonetti PJ, Marteyn BS. 2016. Shigella Diversity and Changing
437 Landscape: Insights for the Twenty-First Century. Front Cell Infect Microbiol 6:45.

438 3. Khalil IA, Troeger C, Blacker BF, Rao PC, Brown A, Atherly DE, Brewer TG, Engmann
439 CM, Houpt ER, Kang G, Kotloff KL, Levine MM, Luby SP, MacLennan CA, Pan WK,
440 Pavlinac PB, Platts-Mills JA, Qadri F, Riddle MS, Ryan ET, Shoultz DA, Steele AD,
441 Walson JL, Sanders JW, Mokdad AH, Murray CJL, Hay SI, Reiner RC. 2018. Morbidity
442 and mortality due to shigella and enterotoxigenic Escherichia coli diarrhoea: the Global
443 Burden of Disease Study 1990–2016. The Lancet Infectious Diseases 18:1229–1240.

444 4. Kotloff KL, Riddle MS, Platts-Mills JA, Pavlinac P, Zaidi AKM. 2018. Shigellosis. The

445 Lancet 391:801–812.

446 5. Mattock E, Blocker AJ. 2017. How Do the Virulence Factors of Shigella Work Together
447 to Cause Disease? Front Cell Infect Microbiol 7:64.

448 6. Schnupf P, Sansonetti PJ. 2019. Shigella Pathogenesis: New Insights through Advanced
449 Methodologies. Microbiology Spectrum 7:7.2.28.

450 7. Cervantes-Rivera R, Tronnet S, Puhar A. 2020. Complete genome sequence and
451 annotation of the laboratory reference strain Shigella flexneri serotype 5a M90T and
452 genome-wide transcriptional start site determination. BMC Genomics 21:285.

453 8. Datsenko KA, Wanner BL. 2000. One-step inactivation of chromosomal genes in
454 Escherichia coli K-12 using PCR products. PNAS 97:6640–6645.

455 9. Campbell-Valois F-X, Sachse M, Sansonetti PJ, Parsot C. 2015. Escape of Actively
456 Secreting Shigella flexneri from ATG8/LC3-Positive Vacuoles Formed during Cell-To-
457 Cell Spread Is Facilitated by IcsB and VirA. mBio 6:e02567-02514.

458 10. Li Z, Liu W, Fu J, Cheng S, Xu Y, Wang Z, Liu X, Shi X, Liu Y, Qi X, Liu X, Ding J,
459 Shao F. 2021. Shigella evades pyroptosis by arginine ADP-riboxanation of caspase-11.
460 Nature 599:290–295.

461 11. Sidik S, Kottwitz H, Benjamin J, Ryu J, Jarrar A, Garduno R, Rohde JR. 2014. A Shigella
462 flexneri Virulence Plasmid Encoded Factor Controls Production of Outer Membrane
463 Vesicles. G3 (Bethesda) 4:2493–2503.

464 12. Baba T, Ara T, Hasegawa M, Takai Y, Okumura Y, Baba M, Datsenko KA, Tomita M,
465 Wanner BL, Mori H. 2006. Construction of Escherichia coli K-12 in-frame, single-gene

466 knockout mutants: the Keio collection. Mol Syst Biol 2:2006.0008.

467 13. Charpentier E, Doudna JA. 2013. Rewriting a genome. Nature 495:50–51.

468 14. Mali P, Yang L, Esvelt KM, Aach J, Guell M, DiCarlo JE, Norville JE, Church GM. 2013.
469 RNA-guided human genome engineering via Cas9. Science 339:823–826.

470 15. Bikard D, Euler CW, Jiang W, Nussenzweig PM, Goldberg GW, Duportet X, Fischetti
471 VA, Marraffini LA. 2014. Exploiting CRISPR-Cas nucleases to produce sequence-
472 specific antimicrobials. Nat Biotechnol 32:1146–1150.

473 16. Jiang W, Bikard D, Cox D, Zhang F, Marraffini LA. 2013. RNA-guided editing of
474 bacterial genomes using CRISPR-Cas systems. 3. Nature Biotechnology 31:233–239.

475 17. Jiang Y, Chen B, Duan C, Sun B, Yang J, Yang S. 2015. Multigene Editing in the
476 Escherichia coli Genome via the CRISPR-Cas9 System. Appl Environ Microbiol
477 81:2506–2514.

478 18. Komor AC, Kim YB, Packer MS, Zuris JA, Liu DR. 2016. Programmable editing of a
479 target base in genomic DNA without double-stranded DNA cleavage. 7603. Nature
480 533:420–424.

481 19. Gaudelli NM, Komor AC, Rees HA, Packer MS, Badran AH, Bryson DI, Liu DR. 2017.
482 Programmable base editing of A•T to G•C in genomic DNA without DNA cleavage.
483 Nature 551:464–471.

484 20. Nishida K, Arazoe T, Yachie N, Banno S, Kakimoto M, Tabata M, Mochizuki M, Miyabe
485 A, Araki M, Hara KY, Shimatani Z, Kondo A. 2016. Targeted nucleotide editing using
486 hybrid prokaryotic and vertebrate adaptive immune systems. Science 353:aaf8729.

487 21. Banno S, Nishida K, Arazoe T, Mitsunobu H, Kondo A. 2018. Deaminase-mediated
488 multiplex genome editing in Escherichia coli. Nat Microbiol 3:423–429.

489 22. Wang Y, Liu Y, Liu J, Guo Y, Fan L, Ni X, Zheng X, Wang M, Zheng P, Sun J, Ma Y.
490 2018. MACBETH: Multiplex automated Corynebacterium glutamicum base editing
491 method. Metabolic Engineering 47:200–210.

492 23. Bartolomé B, Jubete Y, Martínez E, de la Cruz F. 1991. Construction and properties of a
493 family of pACYC184-derived cloning vectors compatible with pBR322 and its
494 derivatives. Gene 102:75–78.

495 24. Gay P, Le Coq D, Steinmetz M, Berkelman T, Kado CI. 1985. Positive selection
496 procedure for entrapment of insertion sequence elements in gram-negative bacteria. J
497 Bacteriol 164:918–921.

498 25. Tobe T, Sasakawa C, Okada N, Honma Y, Yoshikawa M. 1992. vacB, a novel
499 chromosomal gene required for expression of virulence genes on the large plasmid of
500 Shigella flexneri. Journal of Bacteriology 174:6359–6367.

501 26. Yu H, Wu Z, Chen X, Ji Q, Tao S. 2020. CRISPR-CBEI: a Designing and Analyzing Tool
502 Kit for Cytosine Base Editor-Mediated Gene Inactivation. mSystems 5:e00350-20.

503 27. Bernard P, Gabant P, Bahassi EM, Couturier M. 1994. Positive-selection vectors using the
504 F plasmid ccdB killer gene. Gene 148:71–74.

505 28. Dickerson SK, Market E, Besmer E, Papavasiliou FN. 2003. AID Mediates
506 Hypermutation by Deaminating Single Stranded DNA. Journal of Experimental
507 Medicine 197:1291–1296.

508 29. Kuscu C, Adli M. 2016. CRISPR-Cas9-AID base editor is a powerful gain-of-function
509 screening tool. Nat Methods 13:983–984.

510 30. Luria SE, Delbrück M. 1943. Mutations of Bacteria from Virus Sensitivity to Virus
511 Resistance. Genetics 28:491–511.

512 31. Ghosh A, N. S, Saha S. 2020. Survey of drug resistance associated gene mutations in
513 Mycobacterium tuberculosis, ESKAPE and other bacterial species. Sci Rep 10:8957.

514 32. Allaoui A, Sansonetti PJ, Parsot C. 1993. MxiD, an outer membrane protein necessary for
515 the secretion of the Shigella flexneri lpa invasins. Mol Microbiol 7:59–68.

516 33. Sharma A, Puhar A. 2019. Gentamicin Protection Assay to Determine the Number of
517 Intracellular Bacteria during Infection of Human TC7 Intestinal Epithelial Cells by
518 Shigella flexneri. Bio-protocol 9:e3292–e3292.

519 34. Bahrani FK, Sansonetti PJ, Parsot C. 1997. Secretion of Ipa proteins by Shigella flexneri:
520 inducer molecules and kinetics of activation. Infect Immun 65:4005–4010.

521 35. Bernardini ML, Mounier J, d'Hauteville H, Coquis-Rondon M, Sansonetti PJ. 1989.
522 Identification of icsA, a plasmid locus of Shigella flexneri that governs bacterial intra-
523 and intercellular spread through interaction with F-actin. Proc Natl Acad Sci U S A
524 86:3867–3871.

525 36. Carpenter CD, Cooley BJ, Needham BD, Fisher CR, Trent MS, Gordon V, Payne SM.
526 2014. The Vps/VacJ ABC Transporter Is Required for Intercellular Spread of Shigella
527 flexneri. Infection and Immunity 82:660–669.

528 37. Oaks EV, Wingfield ME, Formal SB. 1985. Plaque formation by virulent Shigella

529 flexneri. Infect Immun 48:124–129.

530 38. Sharma A, Puhar A. 2019. Plaque Assay to Determine Invasion and Intercellular
531 Dissemination of Shigella flexneri in TC7 Human Intestinal Epithelial Cells. Bio-
532 protocol 9:e3293–e3293.

533 39. Allaoui A, Mounier J, Prévost M-C, Sansonetti PJ, Parsot C. 1992. icsB: a Shigella
534 flexneri virulence gene necessary for the lysis of protrusions during intercellular spread.
535 Molecular Microbiology 6:1605–1616.

536 40. Rathman M, Jouirhi N, Allaoui A, Sansonetti P, Parsot C, Tran Van Nhieu G. 2000. The
537 development of a FACS-based strategy for the isolation of Shigella flexneri mutants that
538 are deficient in intercellular spread. Molecular Microbiology 35:974–990.

539 41. Hachani A, Biskri L, Rossi G, Marty A, Ménard R, Sansonetti P, Parsot C, Van Nhieu GT,
540 Bernardini ML, Allaoui A. 2008. IpgB1 and IpgB2, two homologous effectors secreted
541 via the Mxi-Spa type III secretion apparatus, cooperate to mediate polarized cell
542 invasion and inflammatory potential of Shigella flexenri. Microbes and Infection
543 10:260–268.

544 42. Graffeuil A, Guerrero-Castro J, Assefa A, Uhlin BE, Cisneros DA. 2022. Polar
545 mutagenesis of polycistronic bacterial transcriptional units using Cas12a. Microb Cell
546 Fact 21:139.

547 43. Fels U, Gevaert K, Van Damme P. 2020. Bacterial Genetic Engineering by Means of
548 Recombineering for Reverse Genetics. Frontiers in Microbiology 11:2161.

549 44. Brochado AR, Typas A. 2013. High-throughput approaches to understanding gene
550 function and mapping network architecture in bacteria. Current Opinion in

551 Microbiology 16:199–206.

552 45. Freed NE, Bumann D, Silander OK. 2016. Combining Shigella Tn-seq data with gold-
553 standard E. coli gene deletion data suggests rare transitions between essential and non-
554 essential gene functionality. BMC Microbiology 16:203.

555 46. Wang L, Xue W, Yan L, Li X, Wei J, Chen M, Wu J, Yang B, Yang L, Chen J. 2017.
556 Enhanced base editing by co-expression of free uracil DNA glycosylase inhibitor. Cell
557 Res 27:1289–1292.

558 47. Bridges BA. 2001. Hypermutation in bacteria and other cellular systems. Phil Trans R
559 Soc Lond B 356:29–39.

560 48. Sternberg SH, Redding S, Jinek M, Greene EC, Doudna JA. 2014. DNA interrogation by
561 the CRISPR RNA-guided endonuclease Cas9. Nature 507:62–67.

562 49. Mateus A, Shah M, Hevler J, Kurzawa N, Bobonis J, Typas A, Savitski MM. 2021.
563 Transcriptional and Post-Transcriptional Polar Effects in Bacterial Gene Deletion
564 Libraries. mSystems 6:e00813-21.

565 50. Hove-Jensen B. 2008. Two-step method for curing Escherichia coli of ColE1-derived
566 plasmids. Journal of Microbiological Methods 72:208–213.

567 51. Wang T, Wei JJ, Sabatini DM, Lander ES. 2014. Genetic screens in human cells using the
568 CRISPR-Cas9 system. Science 343:80–84.

569 52. Kleinstiver BP, Prew MS, Tsai SQ, Topkar VV, Nguyen NT, Zheng Z, Gonzales APW, Li
570 Z, Peterson RT, Yeh J-RJ, Aryee MJ, Joung JK. 2015. Engineered CRISPR-Cas9
571 nucleases with altered PAM specificities. Nature 523:481–485.

572 53. Povolotskaya IS, Kondrashov FA, Ledda A, Vlasov PK. 2012. Stop codons in bacteria are
573 not selectively equivalent. Biology Direct 7:30.

574 54. McKenzie GJ, Craig NL. 2006. Fast, easy and efficient: site-specific insertion of
575 transgenes into Enterobacterial chromosomes using Tn7 without need for selection of
576 the insertion event. BMC Microbiol 6:39.

577 55. Tadala L, Langenbach D, Dannborg M, Cervantes-Rivera R, Sharma A, Vieth K,
578 Rieckmann LM, Wanders A, Cisneros DA, Puhar A. 2022. Infection-induced membrane
579 ruffling initiates danger and immune signaling via the mechanosensor PIEZO1. Cell
580 Reports 40:111173.

581 56. García-Nafría J, Watson JF, Greger IH. 2016. IVA cloning: A single-tube universal
582 cloning system exploiting bacterial In Vivo Assembly. Sci Rep 6:27459.

583 57. Inoue H, Nojima H, Okayama H. 1990. High efficiency transformation of Escherichia
584 coli with plasmids. Gene 96:23–28.

585 58. Clerc P, Sansonetti PJ. 1987. Entry of Shigella flexneri into HeLa cells: evidence for
586 directed phagocytosis involving actin polymerization and myosin accumulation. Infect
587 Immun 55:2681–2688.

588 59. 2008. Cytoplasmic targeting of IpaC to the bacterial pole directs polar type III secretion
589 in Shigella. The EMBO Journal 27:447–457.

590 60. Cervantes-Rivera R, Puhar A. 2020. Whole-genome Identification of Transcriptional Start
591 Sites by Differential RNA-seq in Bacteria. Bio-protocol 10:e3757–e3757.

592 61. Zhou K, Zhou L, Lim Q ’En, Zou R, Stephanopoulos G, Too H-P. 2011. Novel reference

genes for quantifying transcriptional responses of Escherichia coli to protein overexpression by quantitative PCR. BMC Molecular Biology 12:18.

Figure legends

Figure 1: Overview of the CRISPR-Cas guided base editing method.

(A) Generation of mutants using *mCherry* as example. After co-transformation with pnCas9-AID and pgRNA, expression of Cas9-AID and a specific sgRNA introduces a premature stop codon in the target sequence. The PAM and the editable window are underlined with the target C nucleotide shown in red. (B) Maps of plasmids pgRNA_AT and pnCas9-AID used for mutagenesis in *E. coli* and *S. flexneri*. (C) Output from CRISPR-CBEI for *mCherry* and (D) the general scheme for high-efficiency cloning of the spacers determined by CRISPR-CBEI.

Figure 2: Mutagenesis of chromosomally encoded *mCherry* in *E. coli* and *S. flexneri*

(A) Schematic representation of the six different conditions (plasmid combinations), numbered from 1-6, used in the experiment. (B) Mutation frequency in *E. coli* and (C) *S. flexneri*, determined as the ratio of the number of non-fluorescent (mutant) colonies to the total number of colonies, after 2 hours of mutagenesis with or without IPTG induction. The numbers on the X-axis correspond to the conditions represented in (A). Each dot represents a technical replicate and is color-coded to represent a biological replicate. The bars represent the median of three independent experiments. Statistical significance was determined by performing two-way ANOVA followed by Sidák's multiple comparison tests to determine the significance of each condition with respect to control conditions (condition 1) and to determine the significance of IPTG addition (ns – not significant, *$P<0.0332$, **$P<0.0021$, ***$P<0.0002$, ****$P<0.0001$). (D) Phenotypic determination of loss of fluorescence in *E.*

coli and (E) *S. flexneri*. Representative visible (Vis) and fluorescence (Flu) images of colonies obtained by spotting logarithmic dilutions of induced (IPTG+) or not induced (IPTG-) cultures, after 2 hours. The numbers 1-6 correspond to the conditions represented in (A).

Figure 3: Comparison of expression from pgRNA and pnCas9-AID in *E. coli* and *S. flexneri*.

(A) Comparison of sfGFP fluorescence from pgRNA-(R)-GFP in *E. coli* and *S. flexneri*::*mScarlet*. Fluorescence and OD_{600} of bacterial cultures were measured simultaneously in a multimode plate reader and the ratio (corrected fluorescence) was determined for each time point. Fold change in fluorescence was determined as a ratio of corrected fluorescence of *E. coli* and *S. flexneri::mScarlet* at each time point. (B) Representative image of a 50:50 mixture of the cultures as in (A) taken with a fluorescence microscope. The arrowhead denotes a representative *S. flexneri* bacterium and the asterisk marks a representative *E. coli* bacterium. (C) Quantification of fluorescence relative to the mean of *E. coli* fluorescence. The horizontal line represents the median. Each dot represents a technical replicate (fluorescent bacterium in one representative image) and is color coded to represent a biological replicate (image taken on different days). Statistical significance was determined by performing one-way ANOVA followed by Tukey's multiple comparison tests (ns – not significant, *P<0.0332, **P<0.0021, ***P<0.0002, ****P<0.0001). (D) Expression of Cas9-AID fusion protein, determined by immunodetection using anti-Cas9 antibody. Mutagenesis of *mCherry*, guided by sgRNA_m2, was performed simultaneously. The outcome of the mutagenesis is shown as visible (Vis) and fluorescence (Flu) images of colonies obtained by spotting 10^{-5} dilution of the cultures.

Figure 4: Nalidixic acid resistance assay to compare the frequency of guided and random mutations.

642 (A) Schematic representation of the four different conditions (plasmid combinations),
643 numbered 1-4, used in the experiment. (B) Mutation frequency, determined as the ratio of the
644 number of nalidixic acid resistant (mutant) colonies to the total number of colonies, after 2
645 hours of mutagenesis with and without IPTG induction. The numbers on the X-axis
646 correspond to the conditions represented in (A). Each dot represents a technical replicate and
647 is color-coded to represent a biological replicate. In some technical replicates, the mutation
648 frequency was below the limit of observation ($1x10^{-9}$) as spotting high concentrations of the
649 bacterial culture resulted in a bacterial mass, instead of distinct antibiotic resistant colonies.
650 The bars represent the median of three independent experiments. Statistical significance was
651 determined by performing two-way ANOVA followed by Sidák's multiple comparison tests
652 for each condition with respect to the control (condition 1) and for IPTG addition (ns – not
653 significant, **P*<0.0332, ***P*<0.0021, ****P*<0.0002, *****P*<0.0001).

654 **Figure 5: CRISPR/Cas-guided mutagenesis of characterized *S. flexneri* genes and**
655 **assessment of their phenotype.**

656 (A) Representation of the STOP codons (highlighted in red) introduced by base-editing. The
657 total length of the gene is indicated by a line and the red mark indicates the location of the
658 mutable target site. (B) Schematic representation of the gentamicin protection assay used to
659 assess the invasiveness of *Shigella*. (C) Invasiveness of *S. flexneri* WT and *mxiD(Q323X)*,
660 determined by the number of bacterial CFU used to infect TC7 cells (input) and the number
661 of bacterial CFU that were successful at invading them (output). In case of *S. flexneri*
662 *mxiD(Q323X)*, the CFU count was not above the technical limit of observation (10^2 CFU/ml).
663 (D) SDS-PAGE gel showing the total secreted proteins precipitated from the supernatants of
664 indicated bacterial cultures after induction of secretion by Congo red. BSA was used as a
665 control for protein precipitation. (E) Invasiveness of WT, *icsA(Q59X)*, and *vacJ(Q90X) S.*
666 *flexneri* determined by the gentamicin protection assay. (F) Schematic representation of the

plaque formation assay. (G) Intracellular dissemination of WT and mutant *S. flexneri* determined by plaque formation assay. The images depict the stained monolayer of TC7 cells in a 6-well plate with the plaques seen as zones of clearance. (H) Invasiveness of WT and the two strains of *S. flexneri icsB* mutants determined by gentamicin protection assay. (I) Measurement of the diameters of the plaques from one representative plaque formation assay. In all the plots, each dot represents a technical replicate and is color-coded to represent a biological replicate. The bars represent the median of three independent experiments (except in (I)). Statistical significance was determined by performing two-way ANOVA followed by Sidák's multiple comparison test (ns – not significant, **P*<0.0332, ***P*<0.0021, ****P*<0.0002, *****P*<0.0001).

Figure 6: Assessment of polar effects of base-edited mutations.

(A) Representation of the *icsB* operon. The red vertical lines represent the site of introduction of STOP codon in *icsB* and *ipgB* genes. The small horizontal black lines represent the amplicon used to determine the mRNA abundance by qPCR. (B) Normalized (to *cysG* and *hcaT*) expression of *icsB*, *ipgB*, and *ipaC* genes in different mutant strains. Each dot represents a single amplicon and is color-coded to represent a biological replicate. Statistical significance was determined by performing a two-way ANOVA and Holm-Sidák's multiple comparison tests compared to WT (ns – not significant, **P*<0.0332, ***P*<0.0021, ****P*<0.0002, *****P*<0.0001). (C) SDS-PAGE gel showing the secreted proteins (labelled with arrowheads) precipitated from the supernatants of indicated bacterial cultures after induction of secretion by Congo red. (D) Invasiveness of *S. flexneri* strains, determined by the number of bacterial CFU used to infect TC7 cells (input) and the number of bacterial CFU that were successfully invaded (output). Each dot represents a technical replicate and is color-coded to represent a biological replicate. The bars represent the median of three biological replicates. Statistical significance was determined by performing a two-way

692 ANOVA followed by Sidák's multiple comparison test compared to WT (ns – not significant,
693 *P<0.0332, **P<0.0021, ***P<0.0002, ****P<0.0001).

694 ## Tables

695 **Table 1. Details of characterized *S. flexneri* genes that were selected for mutagenesis.**
696 The selected genes are found both on the virulence plasmid and the chromosome. The
697 variation in the number of spacers and their corresponding mutable sites is also mentioned.

Gene	Location	Spacers	Function	Mutant phenotype	Reference
vacJ	Chromosome	Three spacers; same mutable site	Lysis of protrusion during intracellular dissemination	Dissemination defect	(36)
icsA	Virulence plasmid	Two spacers; different mutable sites	Actin-based motility	Dissemination defect	(35)
icsB	Virulence plasmid	Two spacers; different mutable sites	Post-invasion virulence factor	Dissemination defect (?)	(39, 40)
mxiD	Virulence plasmid	One spacer	Structural component of the injectisome	Invasion defect	(32)

698

699 ## Supplementary Material

700 **Supplementary Methods S1.** Detailed methodology of construction of plasmids, strains and
701 cloning guide RNA.

702 **Supplementary Figure S1.** Determination of J23119 promoter activity in *S. flexneri*. (A) The
703 map of pgRNA showing the restriction sites used to clone sfGFP and to obtain pgRNA-(R)-
704 GFP. The sfGFP has a synthetic ribosome binding site and is cloned under the J23119
705 promoter. (B) *S. flexneri* strains carrying pgRNA-X as non-fluorescent control and pgRNA-

706 (R)-GFP streaked on a TSA plate supplemented with carbenicillin (50 μg/ml).

707 **Supplementary Figure S2.** *S. flexneri::mCherry* transformants visualized by Typhoon
708 scanner (GE Healthcare) prior to mutagenesis experiment to verify fluorescence.

709 **Supplementary Figure S3.** (A) Mutation frequency in *E. coli*::*mCherry*, determined as the
710 ratio of the of number of non-fluorescent (mutant) colonies to the total number of colonies,
711 after 4, 6, and 20 hours of mutagenesis with or without IPTG induction. (B) Titer of *E.*
712 *coli*::*mCherry* during mutagenesis determined by counting the colonies spotted after 2, 4, 6,
713 and 20h of mutagenesis with or without IPTG. (C) Mutation frequency in *S.*
714 *flexneri*::*mCherry*, determined as the ratio of the of number of non-fluorescent (mutant)
715 colonies to the total number of colonies, after 4 and 6 hours of mutagenesis with or without
716 IPTG induction. (D) Titer of *S. flexneri*::*mCherry* during mutagenesis determined by
717 counting the colonies spotted after 2, 4, and 6 h of mutagenesis with or without IPTG. The
718 numbers on the X-axis in each graph correspond to the conditions represented in (Fig. 2A).
719 Each dot represents a technical replicate and is color-coded to represent a biological replicate.
720 The bars represent the median of three independent experiments. Statistical significance was
721 determined by performing two-way ANOVA followed by Sidák's multiple comparison tests
722 for of each condition with respect to the control (condition 1) and to determine the
723 significance of for IPTG addition (ns – not significant, *P<0.0332, **P<0.0021,
724 ***P<0.0002, ****P<0.0001).

725 **Supplementary Figure S4:** (A) Microscopic images of 50:50 mixture of *S. flexneri* WT
726 carrying pgRNA-(R)-GFP and *S. flexneri::mScarlet* carrying control plasmid pgRNA-X
727 cultures taken using different filters. (B) Immunodetection of nCas9-AID fusion protein using
728 anti-Cas9 antibody. The left panel is a representative of multiple Western Blots and the right
729 panel is a representative SDS-PAGE gel of the same samples run in parallel. (C) Mutation
730 frequency in *S. flexneri*, determined as the ratio of the number of nalidixic acid resistant

(mutant) colonies to the total number of colonies, after 4 and 6 h of mutagenesis with and without IPTG induction. The numbers on the X-axis correspond to the conditions represented in (Fig. 4A). Each dot represents a technical replicate and is color-coded to represent a biological replicate. In some technical replicates, the mutation frequency was below the technically possible limit of observation ($1x10^{-9}$). The bars represent the median of three independent experiments. Statistical significance was determined by performing two-way ANOVA followed by Sidák's multiple comparison tests for each condition with respect to the control (condition 1) and for IPTG addition (ns – not significant, **P*<0.0332, ***P*<0.0021, ****P*<0.0002, *****P*<0.0001). (D) Normalized (to *cysG* and *hcaT*) expression of *icsB*, *ipgB*, and *ipaC* genes in different mutant strains. Statistical significance was determined by performing (a) a Kruskal-Wallis test (non-parametric) with Dunn's multiple comparison test and (b) One-way ANOVA (parametric) with Dunnett's multiple comparison test. The results are represented as (a)/(b) on each bar (ns – not significant, **P*<0.0332, ***P*<0.0021, ****P*<0.0002, *****P*<0.0001).

Supplementary Figure S5: Overview of the workflow to generate multiple parallel mutations in *Shigella* in high throughput. Cloning the spacer oligos in pgRNA and transformation in *E. coli* DH5α is done on Day 1. The transformants obtained can be inoculated to extract plasmids later on Day 2 or overnight cultures can be made for plasmid extraction on Day 3. pgRNA are transformed on Day 3 and *S. flexneri* colonies carrying both plasmids are selected on Day 4 after overnight incubation. Inoculations can be made to carry out mutagenesis later on the same day (Day 4) or overnight cultures can be prepared for mutagenesis on Day 5. Depending on the incubation, colony PCRs can be performed on Day 5 or Day 6 (the day following mutagenesis).

Supplementary Table S1. Bacterial strains, cells and plasmids used in this study

Supplementary Table S2. Oligonucleotides used in this study

Figure 1

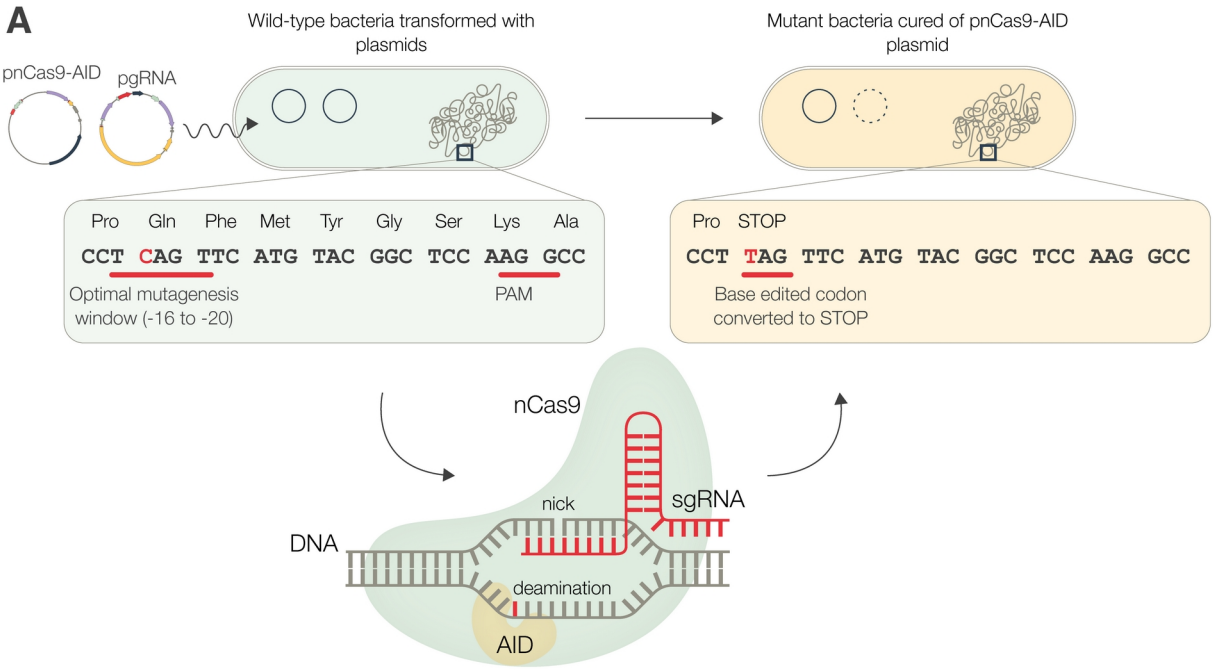

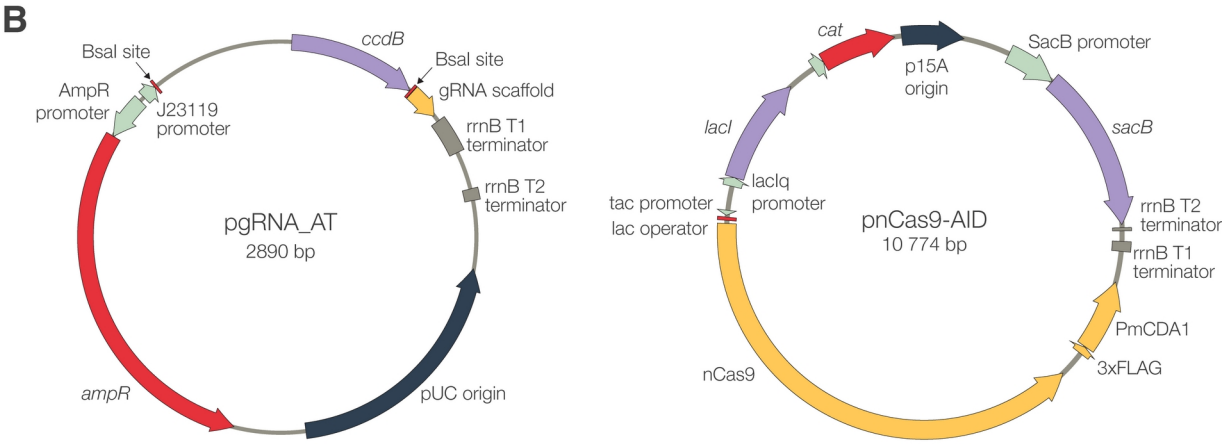

C

CRISPR-CBEI

a web-based designing tool for **C**ytosine**B**ase**E**ditor mediated gene**I**nactivation

ID	Strand	Sequence	Location
1	Plus	CACCCAGACCGCCAAGCTGA	19.55%
2	Minus	TGTCCCAGGCGAAGGGCAGG	26.58%
3	Plus	TCAGTTCATGTACGGCTCCA	28.83%
4	Minus	GCTCCCACTTGAAGCCCTCG	41.35%
5	Minus	CCACTTGAAGCCCTCGGGGA	41.35%
6	Plus	GACCCAGGACTCCTCCCTGC	47.82%
7	Plus	CAGGACTCCTCCCTGCAGGA	47.82%
8	Plus	TGCAGAAGAAGACCATGGGC	59.63%
9	Plus	GCAGAAGAAGACCATGGGCT	59.63%

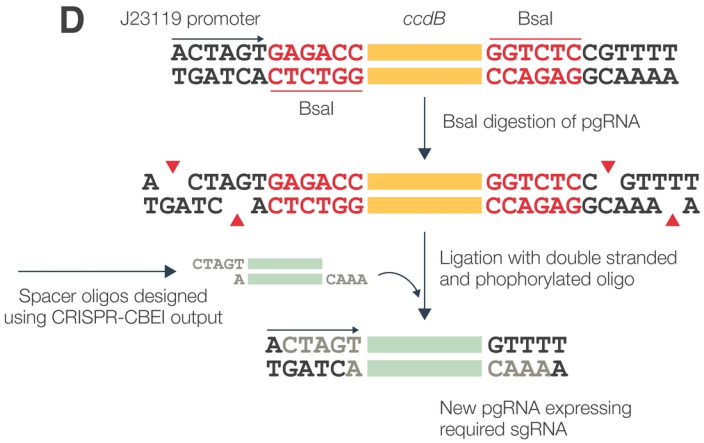

Figure 2

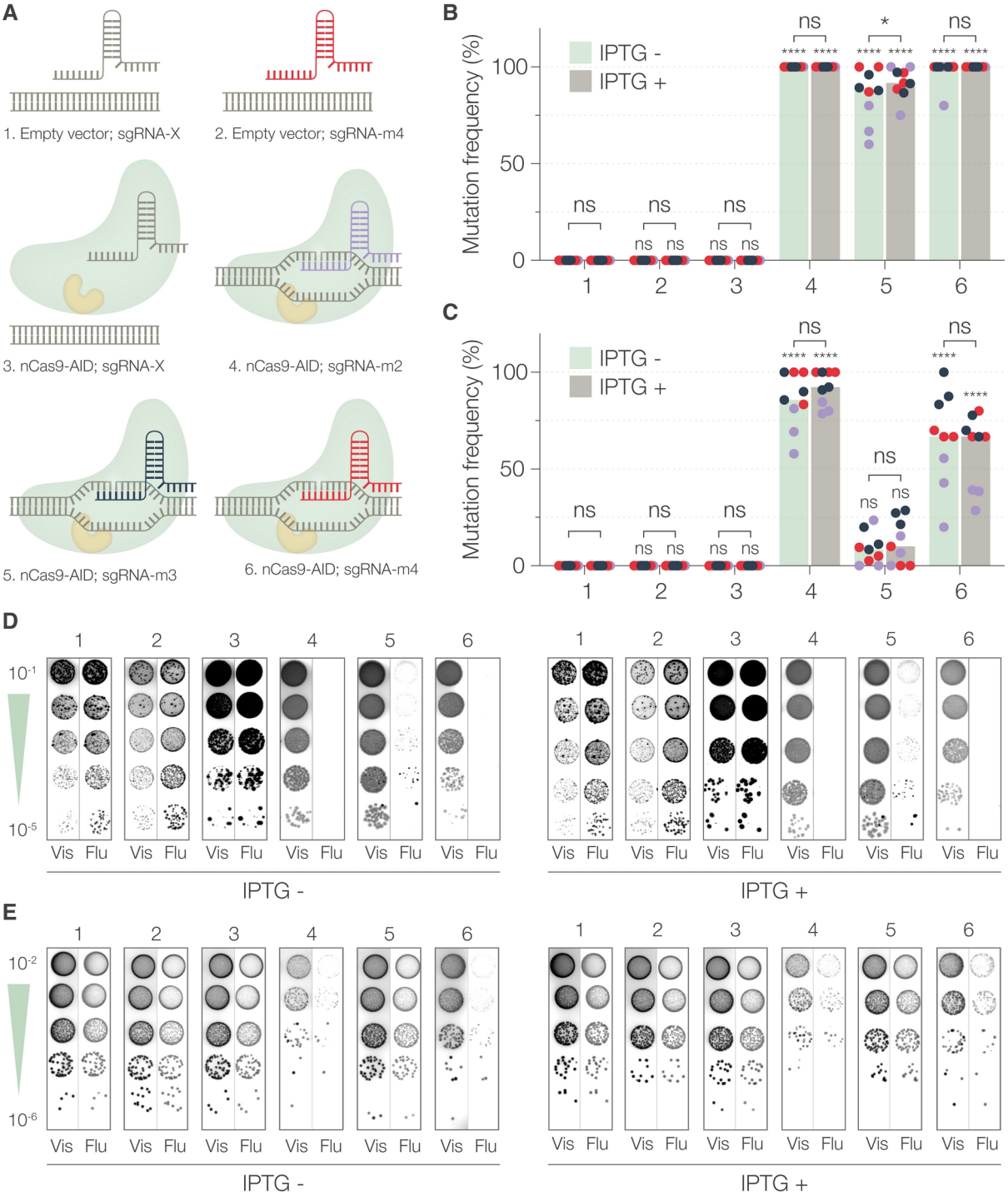
A
1. Empty vector; sgRNA-X
2. Empty vector; sgRNA-m4
3. nCas9-AID; sgRNA-X
4. nCas9-AID; sgRNA-m2
5. nCas9-AID; sgRNA-m3
6. nCas9-AID; sgRNA-m4
B
Mutation frequency (%)
IPTG -
IPTG +
ns
*
****
C
D
E
Vis
Flu
IPTG -
IPTG +

Figure 3

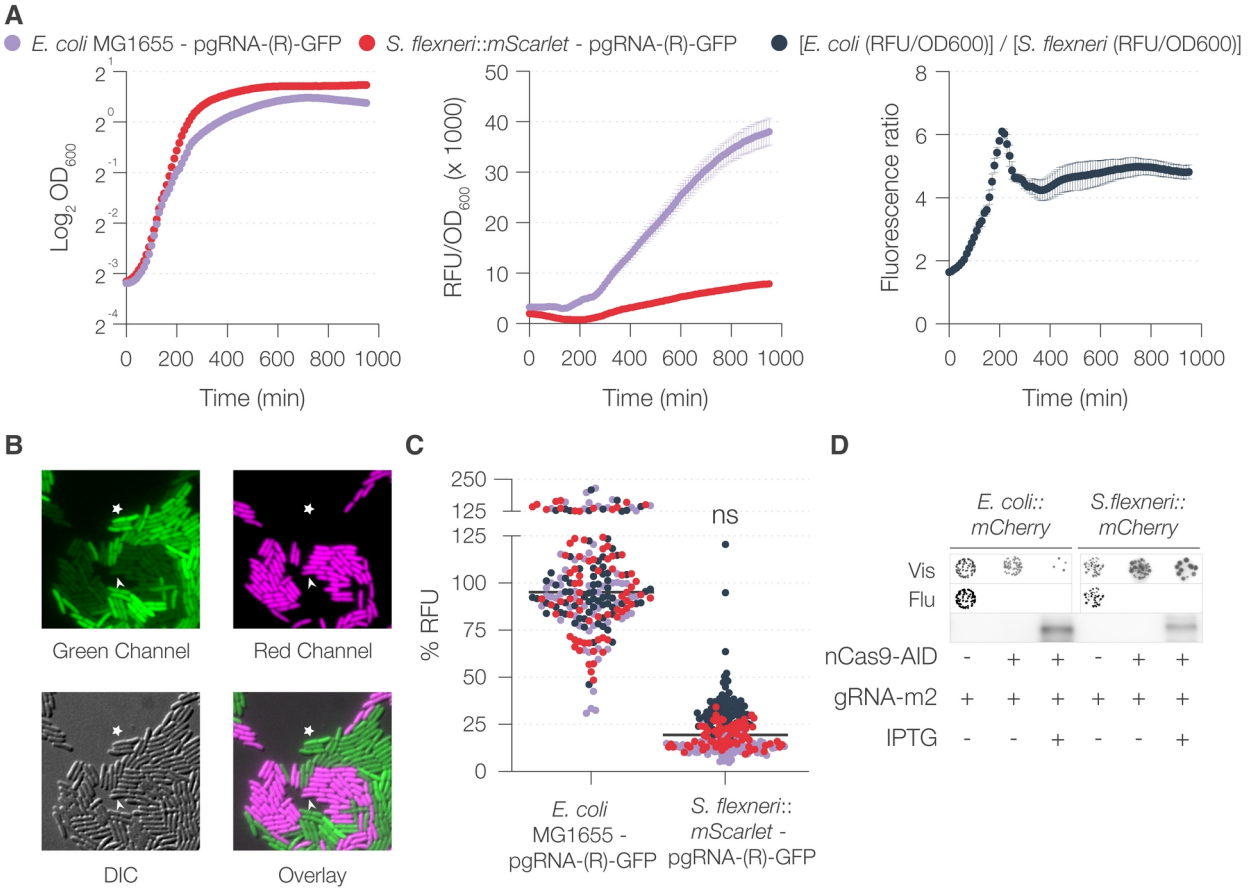
A
E. coli MG1655 - pgRNA-(R)-GFP
S. flexneri::mScarlet - pgRNA-(R)-GFP
[E. coli (RFU/OD600)] / [S. flexneri (RFU/OD600)]
Log2 OD600
RFU/OD600 (x 1000)
Fluorescence ratio
Time (min)
B
Green Channel
Red Channel
DIC
Overlay
C
% RFU
ns
E. coli MG1655 - pgRNA-(R)-GFP
S. flexneri:: mScarlet - pgRNA-(R)-GFP
D
E. coli:: mCherry
S.flexneri:: mCherry
Vis
Flu
nCas9-AID
gRNA-m2
IPTG

Figure 4

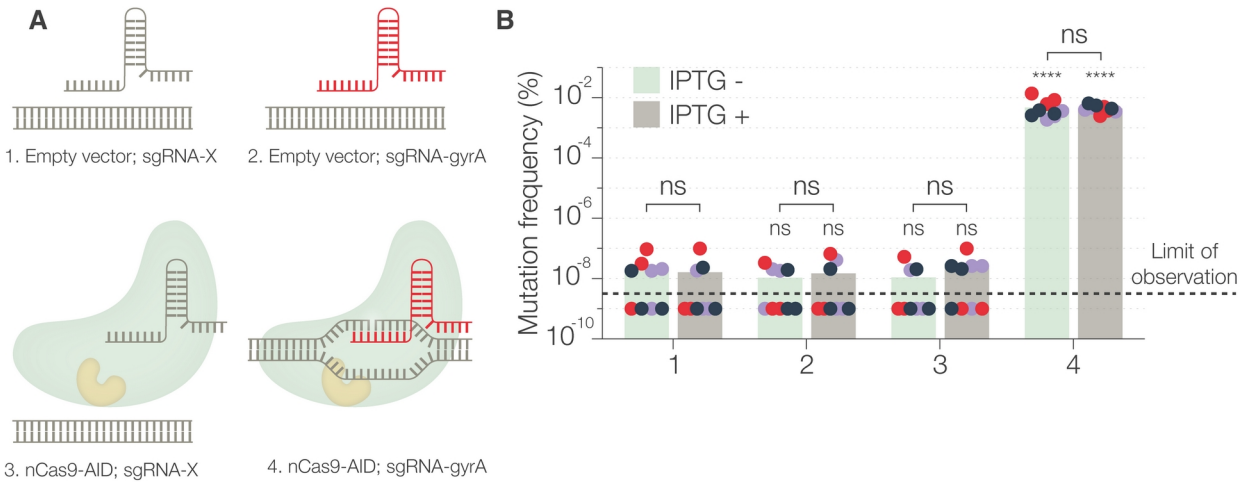
A
1. Empty vector; sgRNA-X
2. Empty vector; sgRNA-gyrA
3. nCas9-AID; sgRNA-X
4. nCas9-AID; sgRNA-gyrA
B
Mutation frequency (%)
IPTG -
IPTG +
ns
****
Limit of observation
1
2
3
4

Figure 5

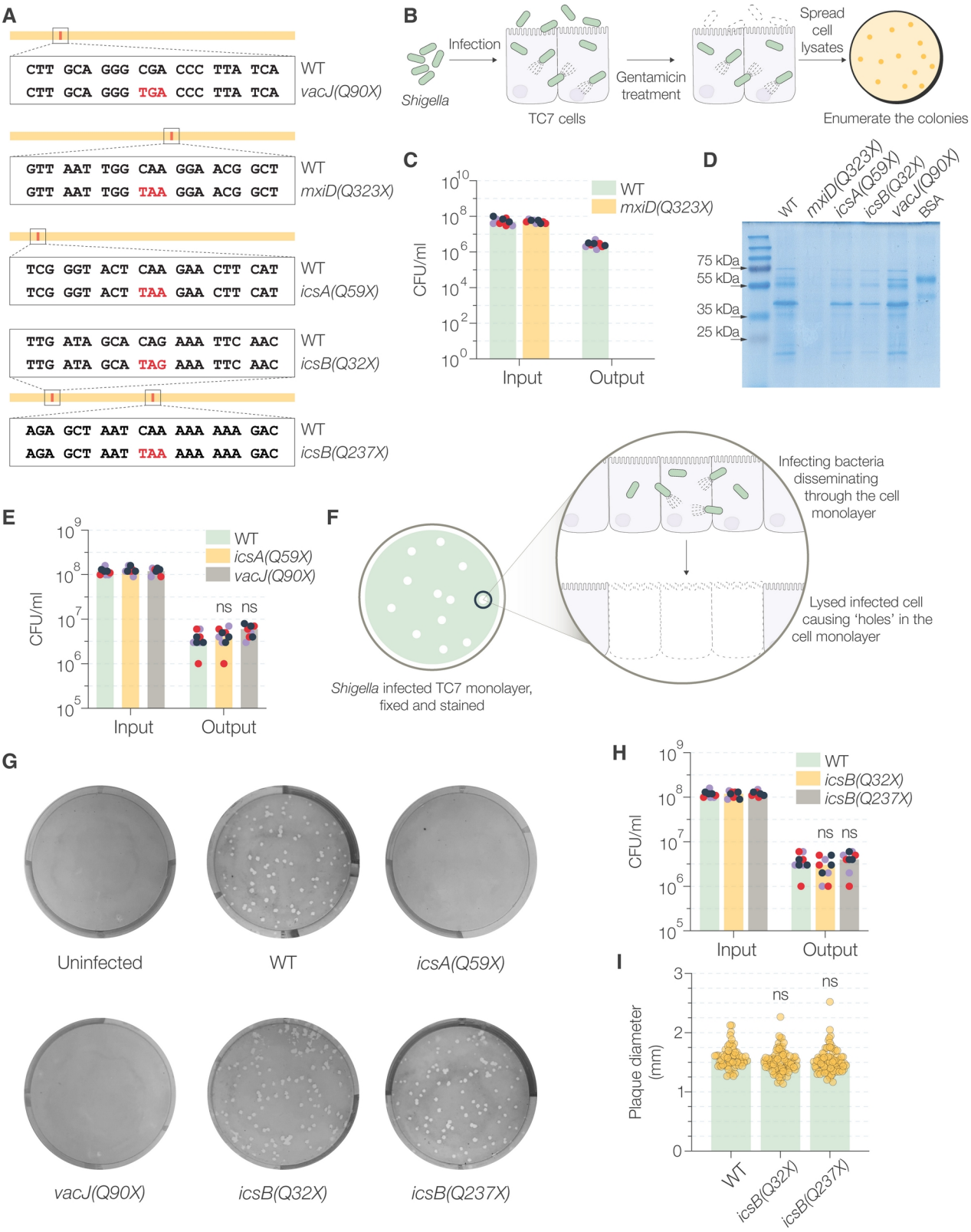
A
CTT GCA GGG CGA CCC TTA TCA
CTT GCA GGG TGA CCC TTA TCA
WT
vacJ(Q90X)
GTT AAT TGG CAA GGA ACG GCT
GTT AAT TGG TAA GGA ACG GCT
WT
mxiD(Q323X)
TCG GGT ACT CAA GAA CTT CAT
TCG GGT ACT TAA GAA CTT CAT
WT
icsA(Q59X)
TTG ATA GCA CAG AAA TTC AAC
TTG ATA GCA TAG AAA TTC AAC
WT
icsB(Q32X)
AGA GCT AAT CAA AAA AAA GAC
AGA GCT AAT TAA AAA AAA GAC
WT
icsB(Q237X)
B
Shigella
Infection
TC7 cells
Gentamicin treatment
Spread cell lysates
Enumerate the colonies
C
CFU/ml
WT
mxiD(Q323X)
Input
Output
D
WT
mxiD(Q323X)
icsA(Q59X)
icsB(Q32X)
vacJ(Q90X)
BSA
75 kDa
55 kDa
35 kDa
25 kDa
E
CFU/ml
WT
icsA(Q59X)
vacJ(Q90X)
ns
ns
Input
Output
F
Infecting bacteria disseminating through the cell monolayer
Lysed infected cell causing 'holes' in the cell monolayer
Shigella infected TC7 monolayer, fixed and stained
G
Uninfected
WT
icsA(Q59X)
vacJ(Q90X)
icsB(Q32X)
icsB(Q237X)
H
CFU/ml
WT
icsB(Q32X)
icsB(Q237X)
ns
ns
Input
Output
I
Plaque diameter (mm)
ns
ns
WT
icsB(Q32X)
icsB(Q237X)

Figure 6

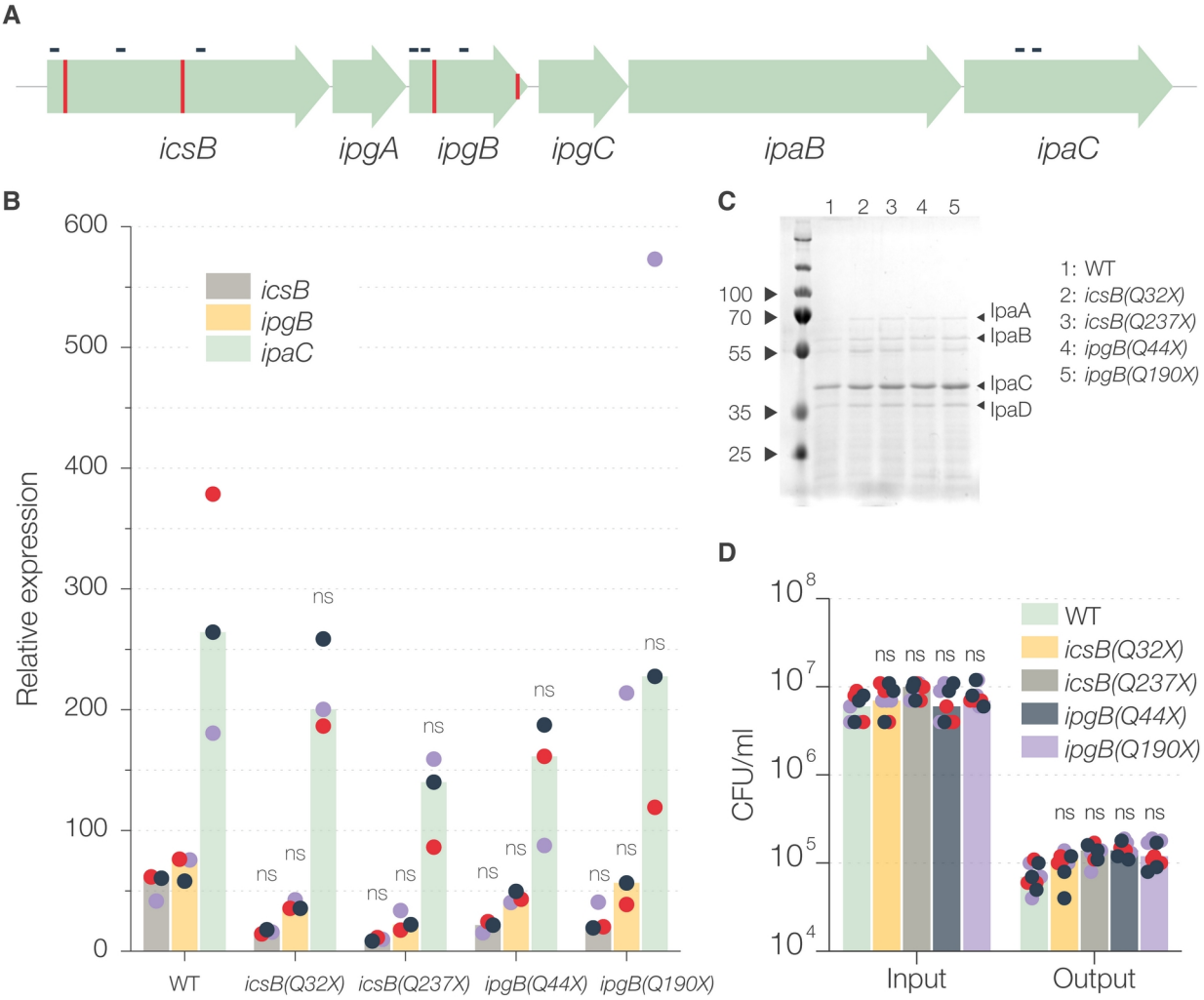
A
icsB
ipgA
ipgB
ipgC
ipaB
ipaC
B
Relative expression
600
500
400
300
200
100
0
icsB
ipgB
ipaC
ns
WT
icsB(Q32X)
icsB(Q237X)
ipgB(Q44X)
ipgB(Q190X)
C
1 2 3 4 5
100
70
55
35
25
IpaA
IpaB
IpaC
IpaD
1: WT
2: icsB(Q32X)
3: icsB(Q237X)
4: ipgB(Q44X)
5: ipgB(Q190X)
D
CFU/ml
10^8
10^7
10^6
10^5
10^4
WT
icsB(Q32X)
icsB(Q237X)
ipgB(Q44X)
ipgB(Q190X)
ns ns ns ns
Input
Output